International Journal of Integrative Research (IJIR)
Vol.4, No.8, 2026: 723-736

Ultrasonic-Assisted Sol–Gel Synthesis of Ag–Zno Nanocomposites for Enhanced in Vitro Sun Protection Factor

Noor Hindryawati[1*], Angela Bergita[2], Husna Syaima[3], Hajar Anuar[4], Teguh Wirawan[5], Eva Marliana[6], Seorja Koesnapadi[7], Irfan Ashari Hiyahara[8]
Universitas Mulawarman, Samarinda
Corresponding Author: Noor Hindryawati hindryawati@gmail.com

A R T I C L E I N F O

Keywords: Ag–Zno Nanocomposite, Zinc Oxide, Silver Nanoparticles, Sol–Gel Synthesis, Ultraviolet Protection, SPF

Received: 4 June
Revised: 25 July
Accepted: 26 August

A B S T R A C T

Sunscreen materials based on inorganic semiconductors are attractive because they can attenuate ultraviolet (UV) radiation through absorption and scattering. This study synthesized Ag–ZnO nanocomposites by an ultrasonic-assisted sol–gel route and evaluated their stability, structural characteristics, particle-size distribution, and in vitro sun protection factor (SPF). $Zn(CH_3COO)_2 \cdot 2H_2O$ was used as the ZnO precursor and $AgNO_3$ was varied at 0.1, 0.4, and 0.9 mM. The resulting materials were characterized by UV–Vis spectroscopy, X-ray diffraction (XRD), scanning electron microscopy (SEM), and particle size analysis (PSA). SPF was estimated from UV–Vis absorbance between 290 and 400 nm using area-under-the-curve calculations. The 0.4 mM Ag formulation [Ag–ZnO(B)] showed the highest crystallinity (71.31%), compared with 69.94% for Ag–ZnO(A) and 67.74% for Ag–ZnO(C). XRD identified hexagonal wurtzite ZnO and face-centered cubic Ag, while SEM showed small Ag-containing particles attached to the ZnO surface together with agglomeration. PSA gave mean particle-size distributions of 75.7 nm for Ag, 325 nm for ZnO, and 730 nm for Ag–ZnO(B), indicating substantial aggregation in the composite dispersion. The synthesized Ag, ZnO, and Ag–ZnO(B) systems remained spectrally stable over four days. The SPF values were 7.126 for Ag, 8.362 for ZnO, and 16.299 for Ag–ZnO(B), corresponding to extra, maximal, and ultra protection categories, respectively, under the classification used in the study. Ag incorporation therefore substantially improved the in vitro UV-protection response of ZnO. Further formulation, dispersion, and safety studies are required before practical cosmetic application

INTRODUCTION

Excessive exposure to solar ultraviolet (UV) radiation can cause erythema, photoaging, oxidative damage, and an increased risk of skin cancer. UV-A radiation occurs approximately at 320–400 nm, whereas UV-B occurs at 290–320 nm and is strongly associated with erythema and direct photobiological damage (Avianka et al., 2022), (Rachmawati et al., 2021). Sunscreens are therefore formulated to attenuate UV radiation by absorption, reflection, or scattering. Inorganic UV filters such as zinc oxide (ZnO) are widely investigated because of their optical stability and broad UV attenuation capability (Rachmawati et al., 2021), (Victoria et al., 2022).

ZnO is a II–VI semiconductor with a band gap of approximately 3.37 eV and a stable hexagonal wurtzite structure at room temperature (Victoria et al., 2022), (Moungsrijun et al., 2017). Its optical properties have made ZnO useful in cosmetic and photoprotective applications. However, the optical response of ZnO is mainly associated with the UV region, motivating modification strategies that extend or strengthen light interaction at longer wavelengths. Silver (Ag) is a particularly interesting modifier because Ag nanoparticles possess strong optical responses, including surface plasmon resonance (SPR), and can contribute to UV shielding through absorption and scattering (Ho et al., 2020), (Ghazwani et al., 2023).

Ag–ZnO hybrid or doped systems have been reported to exhibit modified optical, photocatalytic, and antibacterial properties compared with the parent materials (Karunakaran et al., 2011), (Cuadra et al., 2022), (Alharthi et al., 2020). Ag incorporation can alter the electronic and optical behavior of ZnO and may improve its interaction with UV radiation. In particular, Ag-containing ZnO has been investigated as a photoprotective material because the Ag component can broaden the optical response and enhance photon interaction (Ho et al., 2020), (Bagha et al., 2024), (Abadi et al., 2018).

The sol–gel method provides a relatively simple route for producing oxide materials with controlled chemical composition and high homogeneity (Al-luhaibi & Sendi, 2022), (Karunakaran et al., 2011). Nevertheless, aggregation can occur during particle growth and thermal treatment. Ultrasonic treatment can assist dispersion and disrupt aggregates, making ultrasonic-assisted sol–gel synthesis attractive for preparing metal-oxide nanomaterials (Riwu & Agustini, 2022).

Although Ag–ZnO has been investigated for photocatalytic and antimicrobial applications, its direct evaluation as an SPF-enhancing inorganic sunscreen material remains comparatively less explored in the experimental context of this study. Therefore, this work investigated Ag–ZnO nanocomposites synthesized by an ultrasonic-assisted sol–gel method, using $AgNO_3$ concentrations of 0.1, 0.4, and 0.9 mM. The objectives were to determine the stability of Ag, ZnO, and Ag–ZnO, identify the structural and morphological characteristics of the materials, evaluate particle-size distributions, and compare their in vitro SPF values. The central hypothesis was that Ag modification would increase the UV-protection response of ZnO.

METHODS

Materials and Experimental Design

An experimental laboratory design was used. The study was conducted from February to May 2024 in the Inorganic Chemistry and Basic Chemistry Laboratories, Faculty of Mathematics and Natural Sciences, Universitas Mulawarman, Samarinda, Indonesia. UV–Vis measurements were performed in the Analytical Chemistry Laboratory, Universitas Mulawarman. XRD and SEM analyses were performed at Institut Teknologi Kalimantan, while PSA measurements were conducted at the Center for Nanoscale Science and Nanotechnology, Institut Teknologi Bandung.

The principal reagents were zinc acetate dihydrate [$Zn(CH_3COO)_2 \cdot 2H_2O$], silver nitrate ($AgNO_3$), ammonia/ammonium hydroxide (NH_3/NH_4OH), sodium hydroxide (NaOH), ascorbic acid ($C_6H_8O_6$), trisodium citrate ($Na_3C_6H_5O_7$), and distilled water. The main instruments were a UV–Vis spectrophotometer, Bruker D8 Advance ECO X-ray diffractometer, scanning electron microscope, and Horiba SZ-100 nanoparticle analyzer.

Synthesis of Ag Nanoparticles

Ag nanoparticles were synthesized following the procedure of Yusniar et al. (Yusniar et al., 2021). A 1 mM ascorbic acid solution (100 mL) was adjusted to pH 10 using 3 M NaOH. Subsequently, 12.5 mL of 1 mM $AgNO_3$ and 1 mL of trisodium citrate were added under magnetic stirring. Formation of Ag nanoparticles was indicated by a change from a clear solution to a yellow–brown colloid. Ascorbic acid served as the reducing agent, while citrate contributed to stabilization.

Synthesis of ZnO Nanoparticles

ZnO nanoparticles were prepared with modification of the sol–gel/precipitation procedure reported by Karunakaran et al. (Karunakaran et al., 2011) and Moungsrijun et al. (Moungsrijun et al., 2017). A 0.1 M zinc acetate solution was prepared and 12.5% ammonia solution was added dropwise to pH 7 under constant stirring for 15 min. The mixture was sonicated for 15 min, and the resulting gel was aged overnight. The gel was washed three times with distilled water and separated by centrifugation. The product was dried at 100 °C for 12 h and calcined at 450 °C for 2 h.

Synthesis of Ag–ZnO Nanocomposites

Ag–ZnO nanocomposites were synthesized using 0.1 M zinc acetate and $AgNO_3$ at three concentrations: 0.1 mM [Ag–ZnO(A)], 0.4 mM [Ag–ZnO(B)], and 0.9 mM [Ag–ZnO(C)]. The mixed precursor solutions were treated with 12.5% ammonium hydroxide to pH 7 while stirring for 15 min and then sonicated for 15 min. After overnight aging, the gels were washed three times with distilled water, centrifuged, dried at 100 °C for 12 h, and calcined at 450 °C for 2 h.

Stability Analysis

UV–Vis spectroscopy was used to monitor the optical stability of the Ag, ZnO, and Ag–ZnO dispersions for four consecutive days. The Ag colloid was examined in the 350–500 nm region, ZnO in the 200–400 nm region, and Ag–ZnO in the 250–500 nm region. The material was considered spectrally stable when the characteristic absorption maxima showed no substantial shift during the observation period.

Structural, Morphological, and Particle-Size Characterization

XRD was used to identify crystalline phases and calculate crystallinity. The Bruker D8 Advance ECO diffractometer was used for the measurements. SEM was used to examine surface morphology; approximately 0.1 g of powder was mounted on carbon tape before analysis. PSA measurements were conducted using a Horiba SZ-100 nanoparticle analyzer. A 1 mL sample aliquot was placed in a zeta-potential cuvette for measurement. The particle-size distributions reported here follow the PSA output of the thesis; because PSA measures dispersed/agglomerated populations, these values should not be interpreted as primary crystallite sizes.

In Vitro SPF Determination

SPF activity was determined by UV–Vis spectrophotometry following Ramonah et al. (2022). ZnO and Ag–ZnO samples were prepared by dispersing 0.05 g of powder in 10 mL distilled water. Absorbance was measured from 290 to 400 nm using distilled water as the blank, with three replicate measurements. The thesis states that the spectrophotometer was operated at 2 nm intervals; however, the reported AUC calculation tables use 5 nm intervals. The present manuscript retains the reported calculation procedure and resulting SPF values to preserve the original experimental record. The AUC between adjacent wavelengths was calculated as:

$$AUC_{a-\beta} = [(A_a + A_\beta) / 2] \times (\lambda_\beta - \lambda_a)$$

where A is the measured absorbance and λ is the wavelength. The total AUC was obtained by summing the intervals. The SPF was then calculated as SPF = $10^{[\Sigma AUC/(\lambda_1 - \lambda_0)]}$, where λ_1 = 400 nm and λ_0 = 290 nm. The thesis reports the protection descriptors 'extra,' 'maximal,' and 'ultra'; these descriptors are retained as study-reported categories rather than attributed directly to current FDA labeling. For Indonesian regulatory context, the BPOM classification is low (SPF ≥6 to <15), moderate (≥15 to <30), high (≥30 to <50), and very high (≥50). Importantly, BPOM states that in vitro UV spectrophotometry is a preliminary method for estimating SPF and is not sufficient to establish the SPF value for a commercial cosmetic claim; in vivo testing is the principal standard for such claims (BPOM, 2023).

RESULTS AND DISCUSSION

Formation and Stability of Ag and ZnO Nanoparticles

The Ag synthesis produced a yellow–brown colloid, consistent with the formation of Ag^0 nanoparticles by reduction of Ag^+ with ascorbic acid. The colloid showed a characteristic absorption maximum at approximately 415 nm during the four-day monitoring period, with no substantial spectral displacement. This observation was interpreted in the thesis as evidence of short-term colloidal stability.

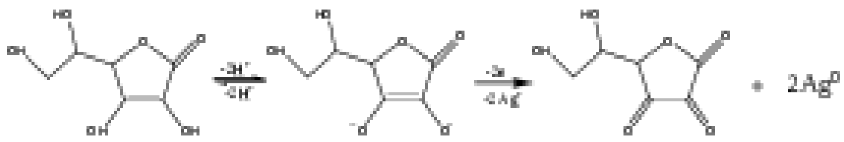

Figure 1. Reaction Scheme For Silver Nanoparticle Formation Using Ascorbic Acid (Adapted From Firdaus Et Al., 2017)

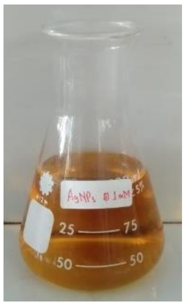

Figure 2. Synthesized Silver Nanoparticle Colloid Obtained Using Ascorbic Acid as the Reducing Agent

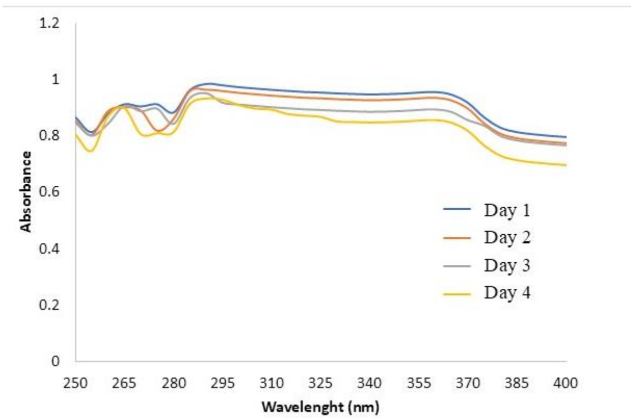

Figure 3. UV–Vis Stability Profile of the Ag Nanoparticle Dispersion Monitored For Four Days

ZnO synthesis produced a white powder with a mass of 1.044 g. The UV–Vis profile showed a characteristic maximum at approximately 290 nm and an absorption region extending toward 360 nm. No substantial displacement of the characteristic maximum was observed during the four-day monitoring period, supporting the short-term spectral stability reported in the thesis.

$$Zn(CH_3COO)_2 \cdot 2H_2O \longrightarrow Zn^{2+} + 2CH_3COO^- + 2H_2O \quad (1)$$

$$NH_4OH \longrightarrow NH_4^+ + OH^- \quad (2)$$

$$Zn^{2+} + 2OH^- \longrightarrow Zn(OH)_2 \quad (3)$$

$$Zn(OH)_2 \longrightarrow ZnO + H_2O \quad (4)$$

Figure 4. Reaction Scheme For Zno Formation From Zinc Acetate Using Ammonium Hydroxide (Adapted From Moungsrijun Et Al., 2017)

Figure 5. Synthesized Zno Powder After Drying and Calcination

3.2 Synthesis and Selection of Ag–ZnO Composition

Three Ag–ZnO formulations were obtained by varying the $AgNO_3$ concentration while maintaining the Zn precursor at 0.1 M. The resulting powders were white and had masses of 1.865 g for Ag–ZnO(A), 1.768 g for Ag–ZnO(B), and 1.548 g for Ag–ZnO(C). The 0.4 mM Ag formulation exhibited the highest crystallinity and was therefore selected for subsequent stability and detailed characterization (Figure 6).

Figure 6. Synthesized Ag–Zno Nanocomposites Prepared with Different $Agno_3$ Concentrations

Table 1. Yield-Related Mass And Crystallinity Of The Ag–Zno Formulations

Material	**$AgNO_3$ concentration**	**Product mass (g)**	**Crystallinity (%)**
Ag–ZnO(A)	0.1 mM	1.865	69.94
Ag–ZnO(B)	0.4 mM	1.768	71.31
Ag–ZnO(C)	0.9 mM	1.548	67.74

Crystallinity increased from 69.94% at 0.1 mM Ag to 71.31% at 0.4 mM Ag, but decreased to 67.74% at 0.9 mM Ag. This non-linear response indicates that the amount of Ag influenced the ordering of the ZnO-based matrix. The intermediate Ag concentration may have provided a more favorable balance between Ag incorporation and ZnO crystal growth, whereas the higher Ag concentration may have increased structural disorder or altered the growth process. Similar concentration-dependent changes in Ag-modified ZnO have been reported for optical and photocatalytic properties (Cuadra et al., 2022), (Alharthi et al., 2020), (Kareem et al., 2022).

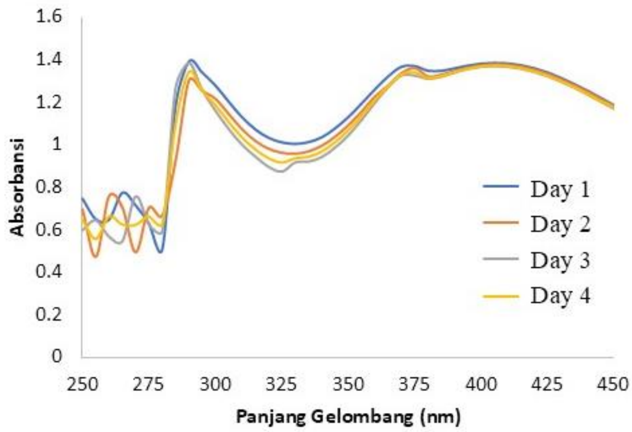

Figure 7. UV–Vis Stability Profile of Ag–Zno(B) Containing 0.4 Mm Ag Monitored for Four Days

Ag–ZnO(B) exhibited two characteristic absorption regions, approximately 290 nm and 405–410 nm. The first is associated with ZnO, whereas the longer-wavelength feature is attributable to the optical response of Ag nanoparticles (Mthana et al., 2022). The small changes in peak position over four days support the conclusion that the selected Ag–ZnO(B) dispersion was spectrally stable over the observation period.

XRD Characterization

The XRD pattern confirmed the coexistence of Ag and ZnO crystalline phases. Ag-related reflections were observed at 2θ = 38.31°, 44.64°, 64.66°, and 77.48°, corresponding to the (111), (200), (220), and (311) planes of face-centered cubic Ag and consistent with JCPDS 04-0783. ZnO reflections appeared at 31.73°, 34.41°, 36.31°, 47.37°, 56.56°, 62.82°, 68.01°, and 69.09°, assigned to the (100), (002), (101), (102), (110), (103), (112), and (201) planes of hexagonal wurtzite ZnO and consistent with JCPDS 36-1451. The coexistence of these phases indicates that Ag acted as a secondary crystalline component in the ZnO matrix (Alharthi et al., 2020), (Kareem et al., 2022).

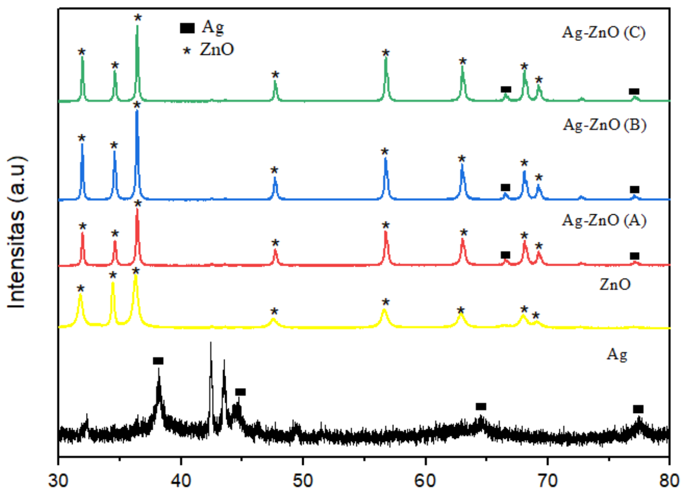

Figure 9. X-Ray Diffraction Pattern of the Ag–Zno Nanocomposite Showing Reflections Assigned to Ag and Hexagonal Wurtzite Zno

The relatively weak Ag reflections in the composite compared with the ZnO reflections can be explained by the comparatively low Ag concentration. The XRD-derived crystallinity values were 17.99% for Ag nanoparticles, 61.32% for ZnO nanoparticles, and 71.31% for Ag–ZnO(B). The higher crystallinity of the selected composite supports its selection for further characterization, although crystallinity alone does not establish cosmetic performance.

SEM Morphology

SEM images showed agglomeration in the Ag, ZnO, and Ag–ZnO samples. In the Ag–ZnO(B) image, small particles were observed attached to the surface of larger ZnO-associated structures, supporting the interpretation that Ag nanoparticles were distributed on the ZnO surface. The non-uniform morphology is consistent with the effect of Ag addition on ZnO crystal growth and with the aggregation commonly reported for Ag–ZnO systems (Cuadra et al., 2022), (Mthana et al., 2022), (Srithar et al., 2017). The relatively high calcination temperature of 450 °C may also have promoted particle necking and aggregation.

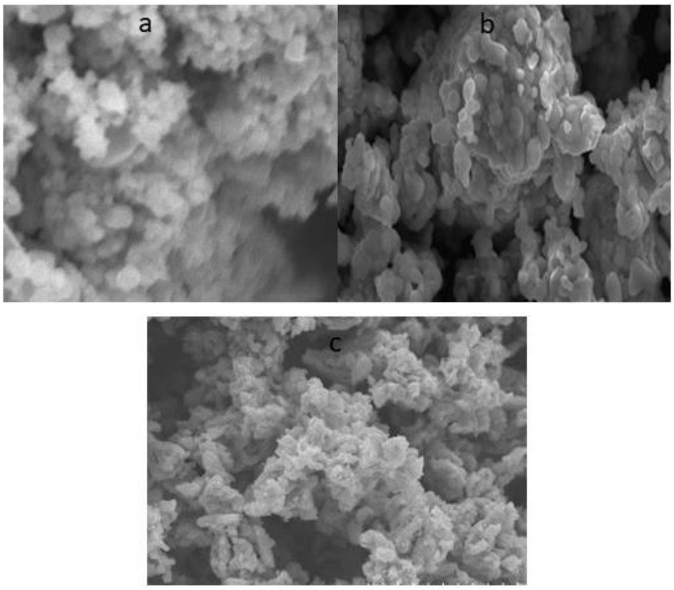

Figure 10. SEM Micrographs Of (A) Ag Nanoparticles, (B) Zno Nanoparticles, And (C) Ag–Zno(B) Nanocomposite

Particle-Size Distribution

PSA measurements produced mean particle-size values of 75.7 nm for Ag, 325 nm for ZnO, and 730 nm for Ag–ZnO(B). The Ag distribution showed two major populations, approximately 15–25 nm and 67–190 nm, suggesting a primary nanoparticle population accompanied by aggregated particles. The ZnO distribution contained three populations at approximately 50–95 nm, 150–350 nm, and 1200–2500 nm. The Ag–ZnO(B) distribution showed two major populations at 150–320 nm and 945–2835 nm. These results indicate substantial aggregation, especially after composite formation. Similar aggregation behavior has been reported for ZnO and Ag–ZnO materials (Mthana et al., 2022), (Bayisa et al., 2023).

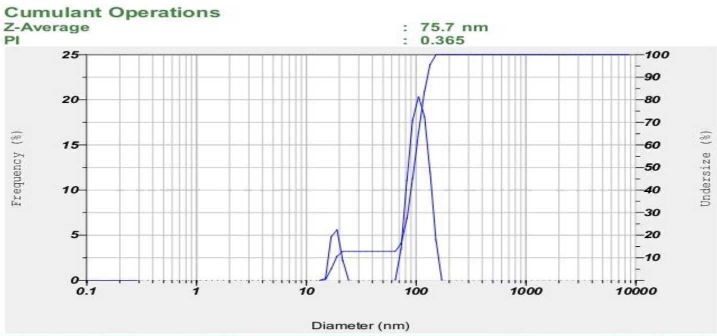

Figure 11. PSA Particle-Size Distribution of the Synthesized Ag Nanoparticles

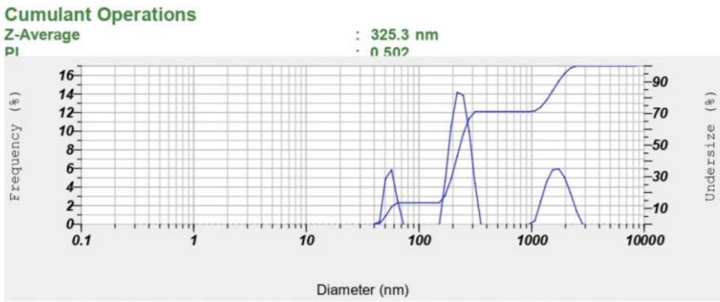

Figure 12. PSA Particle-Size Distribution of the Synthesized Zno Nanoparticles

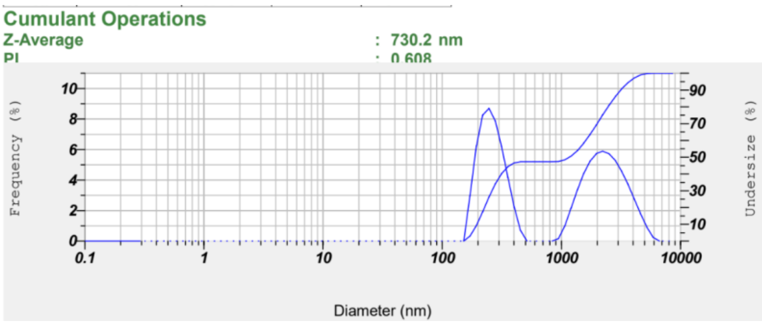

Figure 13. PSA Particle-Size Distribution of the Ag–Zno(B) Nanocomposite

Table 2. PSA-Derived Particle-Size Distributions Of Ag, Zno, And Ag–Zno(B)

Sample	Mean particle size	Main distribution(s)
Ag	75.7 nm	15–25 nm; 67–190 nm
ZnO	325 nm	50–95 nm; 150–350 nm; 1200–2500 nm
Ag–ZnO(B)	730 nm	150–320 nm; 945–2835 nm

An important point for interpretation is that the PSA mean values of ZnO and Ag–ZnO(B) are larger than the conventional 1–100 nm nanoparticle range. The materials can still be described as nanostructured based on their constituent nanophases and SEM/XRD characteristics, but the PSA results demonstrate that the particles formed agglomerated dispersed populations. This distinction is important for future formulation studies because aggregation can influence transparency, UV scattering, sedimentation, and skin-surface behavior.

In Vitro SPF Activity

The SPF results demonstrated a clear enhancement after Ag incorporation into ZnO. Ag nanoparticles produced an SPF of 7.126, ZnO produced 8.362, and Ag–ZnO(B) produced 16.299. The corresponding study-reported descriptors were extra, maximal, and ultra, while the BPOM levels were low, low, and moderate, respectively. The Ag–ZnO(B) SPF was approximately 94.9% higher than the SPF of ZnO alone, indicating a substantially stronger in vitro UV-protection response.

Table 3. In Vitro SPF Values Obtained From Triplicate UV–Vis Measurements

Sample	Mean SPF	Study-reported protection descriptor	BPOM level
Ag	7.126	Extra	Low
ZnO	8.362	Maximal	Low
Ag–ZnO(B)	16.299	Ultra	Moderate

The higher SPF of Ag–ZnO(B) is consistent with the optical behavior observed in the stability measurements. ZnO contributed strong UV-region absorption, while Ag introduced an additional longer-wavelength optical response near 405–410 nm. Ag-containing ZnO systems have been reported to exhibit modified optical behavior and enhanced photon interaction associated with Ag and SPR effects (Bagha et al., 2024), (Abadi et al., 2018). Silver nanoparticles themselves have also been investigated for UV shielding and photoprotective applications (Ho et al., 2020), (Mascarenhas-Melo et al., 2023). The present results therefore support the hypothesis that combining Ag with ZnO can improve the in vitro SPF response relative to either component alone.

Nevertheless, the SPF measurement used an aqueous dispersion and an in vitro UV–Vis method rather than a finished sunscreen formulation or an in vivo skin test. Therefore, the SPF value of 16.299 should be interpreted as an experimental screening result for UV-protective activity, not as a regulatory claim for a commercial sunscreen. BPOM specifically states that in vitro UV spectrophotometry is preliminary for SPF estimation and that in vivo testing is the principal standard for establishing an SPF value for cosmetic labeling (BPOM, 2023). Further work should optimize dispersion stability, assess photostability under prolonged irradiation, evaluate cytotoxicity and oxidative effects, and test the material in a complete topical formulation.

Table 4. Mean Absorbance Values Calculated From the Triplicate Measurements Reported in the Thesis and Used for the AUC-Based SPF Assessment

Wavelength (nm)	Ag mean absorbance	ZnO mean absorbance	Ag–ZnO(B) mean absorbance
290	0.668	0.985	1.400
295	0.620	0.980	1.339
300	0.577	0.974	1.278
305	0.506	0.969	1.202

310	0.438	0.964	1.130
315	0.388	0.960	1.073
320	0.357	0.957	1.033
325	0.345	0.954	1.012
330	0.350	0.951	1.005
335	0.383	0.950	1.013
340	0.452	0.948	1.036
345	0.550	0.949	1.078
350	0.639	0.951	1.131
355	0.731	0.954	1.195
360	0.834	0.956	1.262
365	0.948	0.947	1.323
370	1.081	0.918	1.368
375	1.229	0.866	1.370
380	1.389	0.830	1.349
385	1.580	0.814	1.349
390	1.806	0.806	1.360
395	2.061	0.801	1.373
400	2.335	0.796	1.382

The replicate SPF calculations reported in the thesis gave total AUC values of 93.832, 93.794, and 93.813 for Ag; 101.448, 101.465, and 101.446 for ZnO; and 133.340, 133.334, and 133.337 for Ag–ZnO(B), respectively. The corresponding replicate SPF values were 7.129, 7.123, and 7.126 for Ag; 8.361, 8.364, and 8.361 for ZnO; and 16.300, 16.298, and 16.299 for Ag–ZnO(B). These closely agreeing replicates support the repeatability of the UV–Vis measurement.

CONCLUSION

Ag–ZnO nanocomposites were successfully prepared by an ultrasonic-assisted sol–gel method using zinc acetate dihydrate and $AgNO_3$ concentrations of 0.1, 0.4, and 0.9 mM. All investigated systems showed spectral stability over four days. Among the three composite compositions, Ag–ZnO(B) prepared with 0.4 mM Ag exhibited the highest crystallinity (71.31%). XRD confirmed hexagonal wurtzite ZnO and face-centered cubic Ag phases, while SEM showed Ag-containing particles distributed on the ZnO surface with noticeable agglomeration. PSA gave mean dispersed particle-size values of 75.7 nm for Ag, 325 nm for ZnO, and 730 nm for Ag–ZnO(B), indicating that aggregation was significant in the ZnO-containing systems. The in vitro SPF values were 7.126 for Ag, 8.362 for ZnO, and 16.299 for Ag–ZnO(B). Thus, Ag modification nearly doubled the SPF response of ZnO and produced the highest UV-protection response among the tested materials. The result indicates that Ag–ZnO(B) is a promising candidate for further development as an inorganic UV-protective material; however, formulation optimization, photostability, toxicological evaluation, and skin-safety testing are required before cosmetic application.

Acknowledgments
The authors acknowledge the Department of Chemistry, Faculty of Mathematics and Natural Sciences, Universitas Mulawarman, and the laboratories that supported the synthesis and characterization of the materials.

REFERENCES

Abadi, P. G.-S., Shirazi, F. H., Joshaghani, M., & Moghimi, H. R. (2018). Ag^{+}-promoted zinc oxide [Zn(O):Ag]: A novel structure for safe protection of human skin against UVA radiation. Toxicology in Vitro, 50, 318–327. https://doi.org/10.1016/j.tiv.2018.02.016

Abdelmigid, H. M., Hussien, N. A., Alyamani, A. A., Morsi, M. M., Alsufyani, N. M., & Kadi, H. A. (2022). Green synthesis of zinc oxide nanoparticles using pomegranate fruit peel and solid coffee grounds vs. chemical method of synthesis, with their biocompatibility and antibacterial properties investigation. Molecules, 27(4), 1236. https://doi.org/10.3390/molecules27041236

Alharthi, F. A., Alghamdi, A. A., Al-Zaqri, N., Alanazi, H. S., Alsyahi, A. A., Marghany, A. E., & Ahmad, N. (2020). Facile one-pot green synthesis of Ag–ZnO nanocomposites using potato peel and their Ag concentration dependent photocatalytic properties. Scientific Reports, 10, 20229. https://doi.org/10.1038/s41598-020-77426-y

Al-luhaibi, A. A., & Sendi, R. K. (2022). Synthesis, potential of hydrogen activity, biological and chemical stability of zinc oxide nanoparticle preparation by sol–gel: A review. Journal of Radiation Research and Applied Sciences, 15(3), 238–254. https://doi.org/10.1016/j.jrras.2022.07.008

Avianka, V., Mardhiani, Y. D., & Santoso, R. (2022). Studi pustaka peningkatan nilai SPF (Sun Protection Factor) pada tabir surya dengan penambahan bahan alam. Jurnal Sains dan Kesehatan, 4(1), 79–88. https://doi.org/10.25026/jsk.v4i1.664

Bagha, G., Samavati, K., Naffakh-Moosavy, H., & Matin, L. F. (2024). Controlling surface morphology of Ag-doped ZnO as a buffer layer by dispersion engineering in planar perovskite solar cells. Scientific Reports, 14, 4617. https://doi.org/10.1038/s41598-024-55379-w

Bayisa, Y. M., Bullo, T. A., Hundie, K. B., Akuma, D. A., Gizachew, D. G., & Bultum, M. S. (2023). Ecofriendly green synthesis and characterization of silver zinc oxide nanocomposite using the aqueous leaf extract of Rumex crispus: Evaluation of its antimicrobial and antioxidant activity. Heliyon, 9(5), e16063. https://doi.org/10.1016/j.heliyon.2023.e16063

BPOM RI. (2023). Penjelasan BPOM RI Nomor HM.01.1.2.08.23.33 tanggal 4 September 2023 tentang informasi kosmetik tabir surya (sunscreen) dengan klaim SPF. https://www.pom.go.id/penjelasan-publik/penjelasan-bpom-ri-nomor-hm-01-1-2-08-23-33-tanggal-4-september-2023-tentang-informasi-kosmetik-tabir-surya-sunscreen-dengan-klaim-spf

Cuadra, J. G., Scalschi, L., Vicedo, B., Guc, M., Izquierdo-Roca, V., Porcar, S., Fraga, D., & Carda, J. B. (2022). ZnO/Ag nanocomposites with enhanced antimicrobial activity. Applied Sciences, 12(10), 5023. https://doi.org/10.3390/app12105023

Ghazwani, M., Hani, U., Alqarni, M. H., & Alam, A. (2023). Development and characterization of methyl-anthranilate-loaded silver nanoparticles: A phytocosmetic sunscreen gel for UV protection. Pharmaceutics, 15(5), 1434. https://doi.org/10.3390/pharmaceutics15051434

Ho, Y. Y., Sun, D. S., & Chang, H. H. (2020). Silver nanoparticles protect skin from ultraviolet B-induced damage in mice. International Journal of Molecular Sciences, 21(19), 7082. https://doi.org/10.3390/ijms21197082

Kareem, M. A., et al. (2022). Synthesis, characterization, and photocatalytic application of silver doped zinc oxide nanoparticles. Cleaner Materials, 3, 100041. https://doi.org/10.1016/j.clema.2022.100041

Karunakaran, C., Rajeswari, V., & Gomathisankar, P. (2011). Enhanced photocatalytic and antibacterial activities of sol–gel synthesized ZnO and Ag-ZnO. Materials Science in Semiconductor Processing, 14(2), 133–138. https://doi.org/10.1016/j.mssp.2011.01.017

Mascarenhas-Melo, F., et al. (2023). Inorganic nanoparticles in dermopharmaceutical and cosmetic products: Properties, formulation development, toxicity, and regulatory issues. European Journal of Pharmaceutics and Biopharmaceutics, 192, 25–40. https://doi.org/10.1016/j.ejpb.2023.09.011

Meldayani, R., Iwantono, I., Rini, A. S., & Rati, Y. (2022). Analisa sifat fisis nanopartikel ZnO di-doping Ag yang disintesis menggunakan metode biosintesis. Komunikasi Fisika Indonesia, 19(1), 7–10. https://doi.org/10.31258/jkfi.19.1.7-10

Moungsrijun, S., Sujinnapram, S., & Sutthana, S. (2017). Synthesis and characterization of zinc oxide prepared with ammonium hydroxide and photocatalytic application of organic dye under ultraviolet illumination. Monatshefte für Chemie, 148(7), 1177–1183. https://doi.org/10.1007/s00706-017-1959-z

Mthana, M. S., et al. (2022). Cytotoxicity and antibacterial effects of silver doped zinc oxide nanoparticles prepared using fruit extract of Capsicum chinense. Scientific African, 17, e01365. https://doi.org/10.1016/j.sciaf.2022.e01365

Osmond, M. J., & McCall, M. J. (2010). Zinc oxide nanoparticles in modern sunscreens: An analysis of potential exposure and hazard. Nanotoxicology, 4(1), 15–41. https://doi.org/10.3109/17435390903502028

Rachmawati, P., Sagala, R. J., & Kambira, P. F. A. (2021). Tinjauan pustaka bentuk sediaan tabir surya bahan alam, keamanan dan efektivitas tabir surya.

Ramonah, D., Adhityasmara, D., & Elisa, N. (2022). Penetapan nilai Sun Protection Factor (SPF) daun putri malu (Mimosa pudica Linn.) menggunakan metode spektrofotometer UV-Vis. Pharmauho, 8(2), 20–23.

Riwu, F. K. K. R. U., & Agustini, R. (2022). Effect of mannitol concentration on the stability of encapsulated yeast black rice extract. Indonesian Journal of Chemical Science, 11(2), 136–144. https://doi.org/10.15294/ijcs.v11i2.55200

Sari, D. E. M., & Fitrianingsih, S. (2020). Analisis kadar nilai Sun Protection Factor (SPF) pada kosmetik krim tabir surya yang beredar di Kota Pati secara in vitro. Cendekia Journal of Pharmacy, 4(1), 69–79. https://doi.org/10.31596/cjp.v4i1.81

Srithar, A., Kannan, J. C., & Senthil, T. S. (2017). Preparation and characterization of Ag doped ZnO nanoparticles and its antibacterial applications. Journal of Advances in Chemistry, 13(6), 6273–6279. https://doi.org/10.24297/jac.v13i6.5699

Victoria, J. A., Sugihartono, I., & Isnaeni. (2022). Review zinc oxide (ZnO) nanopartikel sebagai pengobatan kanker. Prosiding Seminar Nasional Fisika, 10, 43–48. https://doi.org/10.21009/03.SNF2022.01.FA.06

Yusniar, Y., Hindryawati, N., & Ruga, R. (2021). Sintesis nanopartikel perak menggunakan reduktor asam askorbat. Prosiding Seminar Nasional Kimia 2021, 187–192.